

University of Groningen

Metabolomics and bioanalysis of terpenoid derived secondary metabolites

Muntendam, Remco

IMPORTANT NOTE: You are advised to consult the publisher's version (publisher's PDF) if you wish to cite from it. Please check the document version below.

Publication date:
2015

[Link to publication in University of Groningen/UMCG research database](#)

Citation for published version (APA):

Muntendam, R. (2015). *Metabolomics and bioanalysis of terpenoid derived secondary metabolites: Analysis of Cannabis sativa L. metabolite production and prenylases for cannabinoid production*. [Thesis fully internal (DIV), University of Groningen].

Copyright

Other than for strictly personal use, it is not permitted to download or to forward/distribute the text or part of it without the consent of the author(s) and/or copyright holder(s), unless the work is under an open content license (like Creative Commons).

The publication may also be distributed here under the terms of Article 25fa of the Dutch Copyright Act, indicated by the "Taverne" license. More information can be found on the University of Groningen website: <https://www.rug.nl/library/open-access/self-archiving-pure/taverne-amendment>.

Take-down policy

If you believe that this document breaches copyright please contact us providing details, and we will remove access to the work immediately and investigate your claim.

Downloaded from the University of Groningen/UMCG research database (Pure): <http://www.rug.nl/research/portal>. For technical reasons the number of authors shown on this cover page is limited to 10 maximum.

Unveiling the active site of the prenyl transferase NphB from *Streptomyces coelicolor*

Alanine scanning of substrate pocket identifies important residues for prenyl transfer of the soluble NphB

Muntendam R., Reis C.R., Koch G., Kayser O.
Manuscript in preparation

Abstract

NphB is a soluble prenyl transferring enzyme acting on an aromatic substrate. The prenyl transfer has been shown to increase the bioactivity of aromatic compounds, such as anti-microbial, anti-oxidant, anti-inflammatory, anti-viral and anti-cancer activities. Despite its importance, the reaction mechanism of this enzyme is poorly understood and only explored using in silico analysis. Based on the reported X-ray crystal structure of the prenyl transferase NphB (1ZB6) in complex with 1,6-dihydroxynaphthalene, geranyl-S-thiol-diphosphate and molecular docking experiments, fourteen active site residues were selected and mutated to the neutral amino acid alanine. Several mutants displayed different features in terms of catalytic efficiency and specificity. Our mutagenesis studies demonstrate the essential role of Asp110, Ser64, Tyr121 and Tyr175, where mutations at these positions resulted in completely inactive mutant enzymes. Interestingly, three single mutations at the active site of NphB yielded mutants (Ser177Ala, Gln295Ala and Gln16Ala) showing an increase in activity when using olivetol as substrate. These results provide a solid basis for further rational improvement of NphB enzyme, targeting both high yield and high product specificity.

Introduction

Aromatic prenylation is the coupling of a prenyl moiety to an aromatic substrate, like polyketides and flavonoids. Many prenylated structures demonstrate a variety of biological activities, such as anti-microbial, anti-oxidant, anti-inflammatory, anti-viral and anti-cancer activities [229-236]. Hence, many studies have been performed to unravel the underlying mechanisms for aromatic prenyl transfer. In *Cannabis sativa*, aromatic prenylation is responsible for the production of cannabigerolic acid (CBGA) which appears to be the key- and rate-limiting step in cannabinoid biosynthesis [94, 105]. Until now, a single aromatic prenyl transferase from *C. sativa* has been cloned and analyzed [275], although it exhibits unfavorable kinetics. Major efforts are focused on the identification of alternative prenyl transferases capable of accepting either olivetol or olivetolic acid as substrate and leading to the synthesis of cannabigerol (CBG) or CBGA respectively. This resulted in the recent identification of a promiscuous prenyl transferase named NphB [109, 256].

NphB is a soluble prenyl transferase from *Streptomyces coelicolor* CL190 and the only candidate, amongst other potentially interesting aromatic prenyl transferases [109, 276, 277], with a solved crystal structure. Structurally, NphB possesses a novel and unique folding, characterized by a repetitive anti-parallel α/β folding (PT barrel). In addition, NphB exhibits promiscuity towards a large amount of substrates [257] including olivetol [256]. As a result of its solved crystal structure and its large substrate promiscuity, NphB constitutes the ideal model for the analysis of prenyl transferases.

Although the structure of NphB has been solved in complex with 1,6-dihydroxynaphthalene (1,6-DHN) and the non-hydrolysable geranyl-S-thiol diphosphate, no extensive mutagenesis studies on the active site amino acids possibly involved in substrate stabilization and the subsequent reaction have been conducted yet. Recently, molecular dynamic studies have been performed in order to identify essential residues and to elucidate the catalytic mechanism [257, 278]. One reporting literature, in addition to our previous work, proposes a putative catalytic mechanism [278, 279]. Although, both identified the reaction to occur in a S_N1 fashion, they differ in the mode of carbocation stabilization. The first one supports the formation of a π -chamber composed of Tyr121, Tyr216 and the substrate (analyzed for 1,6-DHN only) [278]. The second [279] supports carbocation stabilization via either an aromatic amino acid (Trp152 in case of UbiA from *E. coli*) or, in case of NphB, a methionine at position 162. Although both studies identified amino acid residues with importance on

substrate stabilization and in the reaction catalysis, no empirical data support these studies and additionally explore the different catalytic activities observed in NphB.

In this work, we seek to unravel the importance of several active site residues of NphB and their role in the previously described promiscuous activities of NphB. We used 1,6-DHN, naringenin (NAR), olivetolic acid (OLA) and olivetol (OL) as substrates to analyze the differences in catalytic activity and substrate specificity exhibited by the NphB mutants. Our alanine mutagenesis approach led to the identification of several amino acids with putative involvement in substrate catalysis. Interestingly several amino acid replacements led to a significant improvement in catalytic activity, while several amino acid substitutions led to reduced activity or completely inactive enzymes. Our study provides further insight into the catalytic activities and the substrate/product specificity of NphB and therefore furnishes a basis for further enzyme improvement of NphB.

Results

Exploration of active residues for NphB:

Molecular docking experiments were performed using the NphB crystal structure in complex with the substrate 1,6-dihydroxynaphthalene (1,6-DHN) and the non-hydrolysable geranyl-S-thiolo-diphosphate (GSPP), a known inhibitor of prenyl acting enzymes (protein data bank ID: 1ZB6 (**Figure 1A**)). GSPP was replaced by geranyl diphosphate (GPP) and subsequently 1,6-DHN was docked. This experiment resulted in two energetically favorable orientations (**Figure 1B**), differing only slightly from the substrate positioning resolved in the crystal structure. Both olivetol (OL) and naringenin (NAR) were docked within the active cavity based on the coordinates given by 1,6-DHN in the active site of NphB. Previously only 1,6-DHN and NAR [109, 256, 278] had been used in molecular dynamics studies. Analysis of the most energetically favorable poses from all substrates led to the identification of fourteen amino acid residues in the active site that are possibly involved in substrate binding, stabilization or catalysis. The residues selected for mutagenesis were: Val-47; Ser-64; Asp-110; Tyr-121; Phe-123; Thr-126; Gln-161; Tyr-175; Ser-177; Ser-214; Tyr-216; Tyr-288; Val-294 and Gln-295. All residues were replaced with the non-polar non-ionizable alanine.

Analysis of specific activity for alanine mutants:

The selected mutants were purified to homogeneity and analyzed for the activity by using constant substrates, reaction conditions and correcting for used protein amounts. Four different substrates were used in the assays (OL, OLA, NAR and 1,6-DHN), and they were analyzed using UPLC. For all substrates, no background reaction was observed, when BSA replaced the active enzyme without changing the reaction conditions. Using OL resulted in the formation of cannabigerol (CBG), NAR can be prenylated to 7-O-geranyl NAR and 6-geranyl NAR. NphB can synthesize three products when exposed to 1,6-DHN, although with different efficiencies: 5-geranyl-1,6-DHN ($K_{cat} = 5610 \text{ s}^{-1}$) as the major product, followed by 2-geranyl-1,6-DHN ($K_{cat} = 1430 \text{ s}^{-1}$), as second major product, and 4-geranyl-1,6-DHN ($K_{cat} = 430 \text{ s}^{-1}$) as minor product (**Figure 2**).

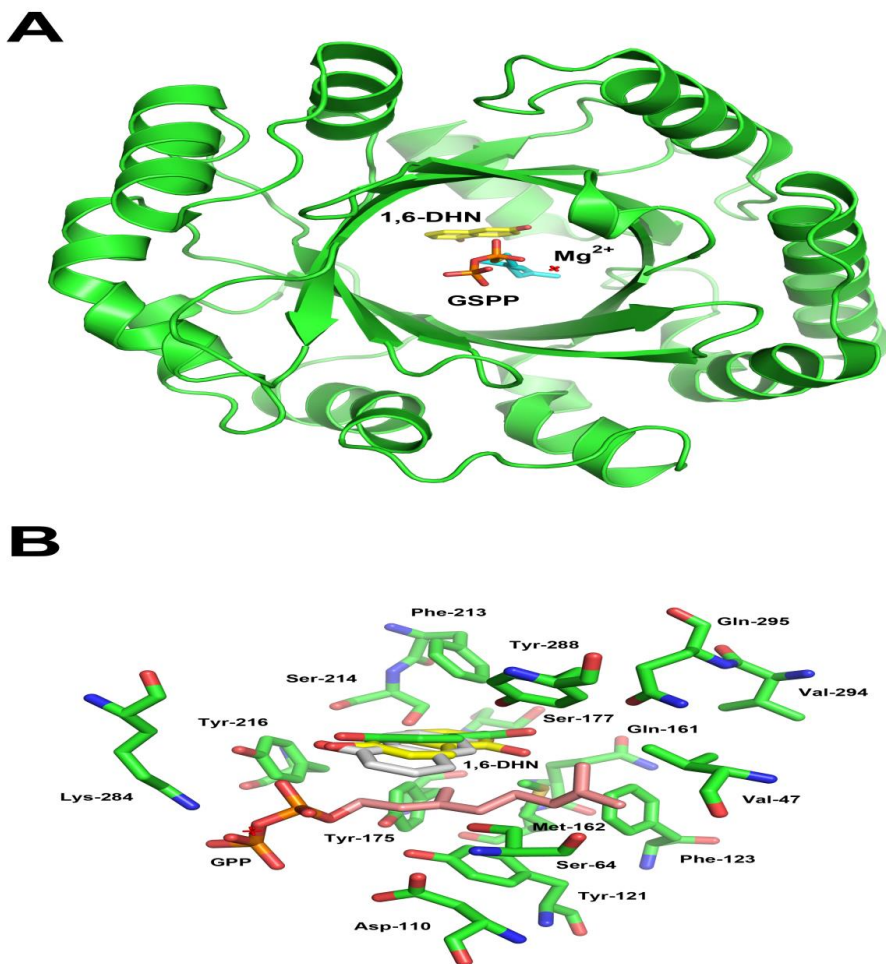


Figure 1: Structure of NphB in complex with GPP (A). Depicted is the structure of wild-type NphB in complex with GSPP and 1,6-DHN (Protein Data Bank accession code: 1ZB6). (B) Molecular docking of 1,6-DHN, after replacement of GSPP with GPP, into the active center of NphB. green sticks, surrounding GPP and 1,6-DHN, indicate chosen residues for mutagenesis. 1,6-DHN from the crystal structure is depicted in green. The two most energetically favorable docked poses obtained by molecular docking are depicted in yellow and pink sticks.

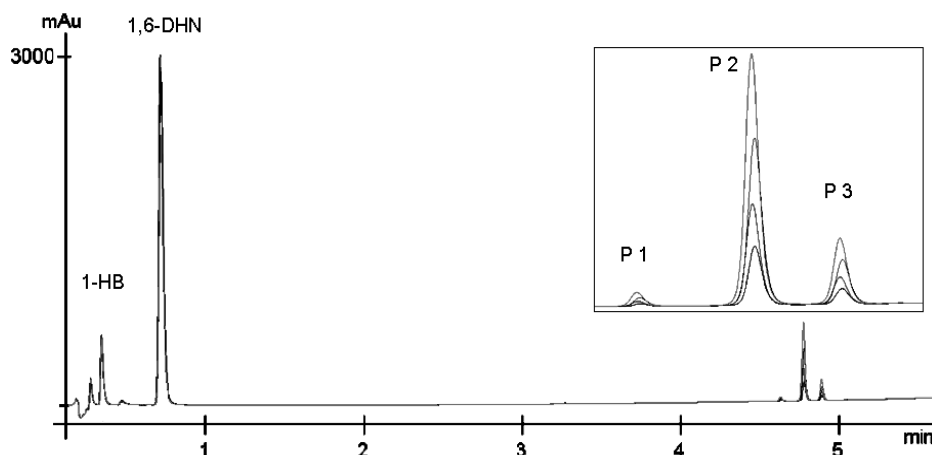


Figure 2: Example of the LC-PDA chromatogram. The box within the figure indicates the production of the three identified products. P1 = 4- geranyl-1, 6-DHN. P2 = 5-geranyl-1,6-DHN. P3 = 2-geranyl-1,6-DHN.

Analysis of activity of the 14 mutants shows that they can be divided according to their effect in substrate stabilization or recognition. Four NphB mutant enzymes (Ser64Ala, Tyr121Ala, Tyr175Ala and Asp110Ala) were completely inactive towards all tested substrates indicating their importance within the active center of NphB.

The results show that the mutants Tyr288Ala, Phe123Ala and Gln295Ala cause a significant change in substrate conversion and specificity. None of the mutants accepted NAR as substrate. Phe123Ala mutant had a 2-fold reduction of activity towards 1,6-DHN and no enzymatic activity could be detected when using OL. The loss of activity towards OL and NAR may indicate the importance of this residue for substrate interaction and/or positioning. The mutant Tyr288Ala displayed a 75 % reduction towards OL. When using 1,6-DHN as substrate, interestingly, Tyr288Ala affected all products, with the formation of the minor product 4-geranyl 1,6-DHN not being observed anymore. The mutant Gln295Ala showed no activity towards NAR. However, only a slight reduction in the specific activity towards 1,6-DHN was observed, with decreasing production levels of the product 2-geranyl-1,6-DHN being most prominent. Also, a 4.6 fold increase was observed when using olivetol.

Notably, the mutants Gln295Ala, Gln161Ala and Ser177Ala led to a significant increase in product accumulation of cannabigerol (CBG) when using OL as substrate, reaching 4.6-, 12.7- and 1.5-fold, respectively. Moreover, the Gln161Ala (**Figure 3**) could produce CBGA in detectable amounts when using olivetolic acid for substrate, while neither the wild type nor the remaining mutants showed activity towards this substrate. In contrast to Gln295Ala, the other two mutants increased prenylation of all tested substrates (**Table 1**).

Altered product specificity could also be observed in the Val294Ala mutant. Although product formation was severely reduced for OL, hardly any effect was observed towards 1,6-DHN. Additionally, the production capacity of the Val294Ala mutant with NAR as substrate was reduced and no *O*-prenylation took place while *C*-prenylation was still present highlighting the importance of this residue regarding substrate specificity towards *O*-prenylation (**Table 2**).

Some of the mutants (Val47Ala and Tyr216Ala) resulted in a severe reduction in the overall product accumulation for the substrates tested. In the Val47Ala mutant, product formation was severely reduced, only 2-geranyl-1,6-DHN could be detected in wild-type levels. The mutant Tyr216Ala, was severely affected in the levels of all products. Although slight enzyme activity was detected, this residual product formation hardly is of any significance.

Interestingly, the mutants Thr126Ala and Tyr214Ala did not show any significant changes in the production levels. Although the product formation for NAR went up with >200 %, the standard deviation has to be taken into consideration, hence carefully interpreting the results. From all mutants tested these positions do not seem to interfere directly with the product formation for both NAR and 1,6-DHN.

Activity analysis of selected mutants:

To analyze the velocity of product formation at various OL substrate concentrations, the mutants Gln295Ala, Gln161Ala and Ser177Ala were selected. These mutants were selected on the basis of increased CBG production levels shown in the previous experiment. Also wild type NphB was used within these experiments, but no CBG could be detected due to the short incubation times and low substrate concentrations used to establish initial velocities. This corresponds to the reported k_{cat} and k_{cat}/K_m values of, 0.027 s^{-1} and $0.052 \text{ M}^{-1} \text{ s}^{-1}$, respectively, indicating a slow reaction rate for the wild type NphB [256].

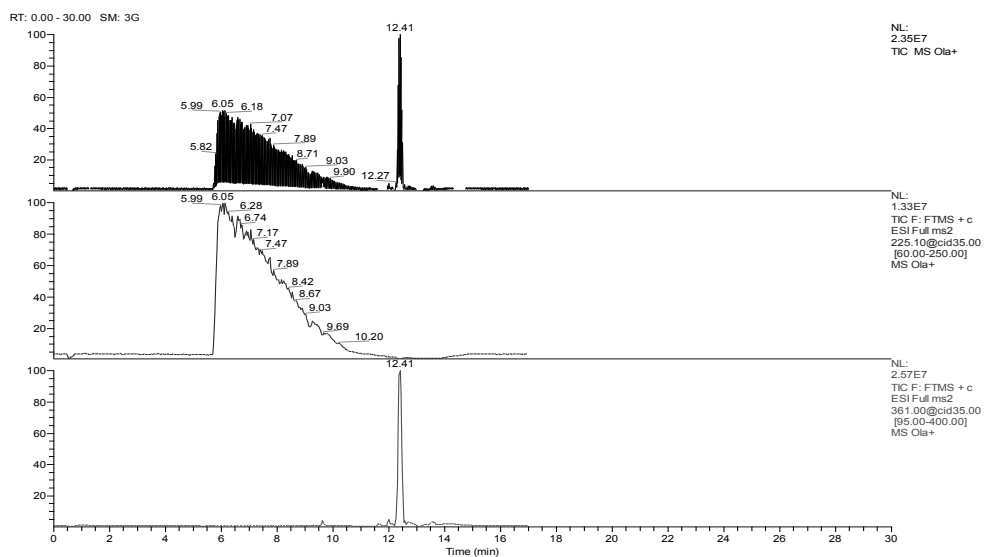


Figure 3: LC-MS analysis for the confirmation of CBGA production by the mutant Gln161Ala. All samples were combined and dried to be able to increase the concentration of the metabolites.

Table 1: Relative product accumulation corrected for enzyme concentration used in the assay. Activity is compared to wild type NphB incubated using 3 different substrates as described within the text.

| Enzyme | 4-G-1,6 DHN (%) | 5-G-1,6 DHN (%) | 2-G-1,6 DHN (%) | 7-o-G- nar (%) | 6-G-nar (%) | CBG (%) | CBGA |
|------------------|-----------------------|-----------------------|-----------------------|-------------------|----------------|------------|-------|
| NphB (WT) | 100±7 | 100±5 | 100±7 | 100±8 | 100±14 | 100±5 | N.D. |
| Asp110Ala | N.D. | 3%±5% | N.D. | N.D. | N.D. | N.D. | N.D. |
| Ser64Ala | N.D. | N.D. | N.D. | N.D. | N.D. | N.D. | N.D. |
| Tyr121Ala | N.D. | N.D. | N.D. | N.D. | N.D. | N.D. | N.D. |
| Tyr175Ala | N.D. | N.D. | N.D. | N.D. | N.D. | N.D.* | N.D.* |
| Phe123Ala | 52±2 | 68±1 | 52±2 | N.D. | N.D. | N.D. | |
| Tyr216Ala | 27±4 | 36±4 | 7±6 | 21±14 | N.D. | N.D.* | N.D.* |
| Ser214Ala | 89±25 | 83±1 | 145±4 | 236±27 | 274±58 | N.D.* | N.D.* |
| Thr126Ala | 122±7 | 110±10 | 116±12 | 126±16 | 146±34 | N.D.* | N.D.* |
| Val294Ala | 74±7 | 101±1 | 104±7 | 0±0 | 91±31 | 12±10 | N.D. |
| Val47Ala | 38±9 | 65±2 | 91±6 | 51±28 | 89±45 | 21±7 | N.D. |
| Tyr288Ala | N.D. | 34±15 | 59±9 | N.D. | N.D. | 24±41 | N.D. |
| Ser177Ala | 187±4 | 345±2 | 467±5 | 151±3 | 194±11 | 150±6 | N.D. |
| Gln295Ala | 98±8 | 104±3 | 75±8 | N.D. | N.D. | 464±1 | N.D. |
| Gln161Ala | 658±4 | 503±4 | 275±4 | 609±9 | 124±19 | 1272±7 | Yes** |

N.D. = Not Detected

* = Olivetol was not tested for these samples

** = No relative comparison could be made due to inactivity of wild type DhnB

The wild type only showed activity (confirmed by LC-MS, using selective ions scanning mode) when incubating for prolonged times. By calculating the velocity in nmol per sec (**Figure 4A**), a clear view can be given on the increased product formation. As mentioned above, the mutant Gln161Ala showed the largest increase in product formation. Similar results were observed for the product formation velocity, clearly indicating an increase in V_{max} , however, the data was not satisfying to estimate the exact kinetic parameters. This can also be observed in the mutants Gln295Ala and Ser177Ala, thus, these two mutations certainly increase the production capacity when using OL as a substrate.

Table 2: Percentage of specific prenylated product from total produced products as an indication of altered product specificity

| | 4-G-1,6 (%) | DHN | 5-G-1,6 (%) | DHN | 2-G-1,6 DHN (%) | 7-o-G-nar (%) | 6-G-nar (%) |
|-------------------|----------------|--------------|----------------|-----|--------------------|---------------|----------------|
| NphB | 5 | | 76 | | 19 | 38 | 62 |
| Asp110Ala | N.D. | | 100 | | N.D. | N.D. | N.D. |
| Ser64Ala | N.D. | | N.D. | | N.D. | N.D. | N.D. |
| Tyr121Ala | N.D. | | N.D. | | N.D. | N.D. | N.D. |
| Tyr175Ala* | N.D. | | N.D. | | N.D. | N.D. | N.D. |
| Phe123Ala | 4 | | 80 | | 16 | N.D. | N.D. |
| Tyr216Ala | 4 | | 91 | | 4 | 100 | N.D. |
| Ser214Ala | 4 | | 66 | | 29 | 35 | 65 |
| Thr126Ala | 5 | | 75 | | 20 | 35 | 65 |
| Val294Ala | 4 | | 76 | | 20 | N.D. | 100 |
| Val47Ala | 3 | | 72 | | 26 | 26 | 74 |
| Tyr288Ala | N.D. | | 69 | | 31 | N.D. | N.D. |
| Ser177Ala | 2 | | 73 | | 25 | 32 | 68 |
| Gln295Ala | 5 | | 80 | | 15 | N.D. | N.D. |
| Gln161Ala | 7 | | 82 | | 11 | 75 | 25 |
| N.D. | = | Not Detected | | | | | |

Additionally, we analyzed the mutants Gln161Ala, Ser177Ala along with wild type NphB for product formation velocity of 5-geranyl-1,6-DHN, as these mutants showed a significant increase in product formation when compared to WT. A clear difference in product velocity can be observed in **Figure 4B**. From the recorded data, it is obvious that an increased V_{\max} forms the basis for the increased activity. The reaction of Gln-161 remains linear while Ser177Ala and WT show a clear platform indicating that the maximum velocity was reached. Therefore, it was not possible to estimate the kinetic parameters for Gln161Ala. Even though a clear increase in V_{\max} is obvious, more enzyme and substrate concentrations need to be tested. For the wild type and Ser177Ala, it was possible to estimate the K_m values, which showed no difference (both 0.2 mM). However the V_{\max} differed tremendously, where 0.8 ABS/sec was observed for the Ser177Ala and only 0.08 Abs/sec was observed for NphB WT. Interestingly no product formation of 2-geranyl-1,6-DHN was observed for Ser177Ala, although, it was observed for Gln161Ala (**Figure 4C and 4D**). A clear platform formation at the highest substrate concentration is present in the Ser177Ala mutant, while a more linear product formation can be seen for Gln161Ala. Data from these experiments indicate that these two mutants can serve as background for more specific mutagenesis to produce an efficient CBG producing enzyme

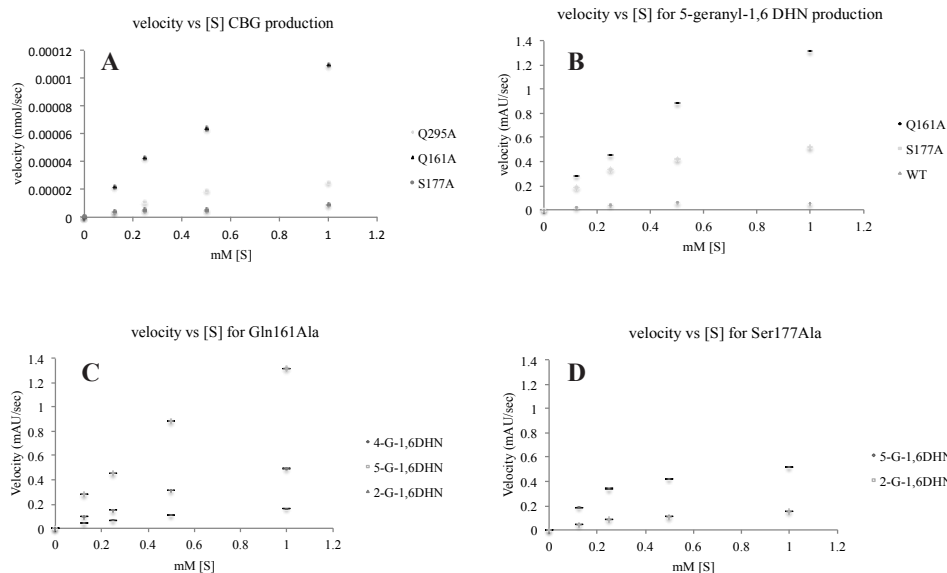


Figure 4: Product formation by selected mutants. **A)** Product formation of CBG is nmol/sec as estimated by external calibration curve using CBG standard. **B)** Velocity of 5-geranyl-1,6-DHN, the major product formed by NphB. **C)** product formation using 1,6-DHN and Gln161Ala. **D)** Product formation using 1,6-DHN and Ser177Ala.

Discussion and future perspectives

Structural information and initial *in silico* docking experiments of NphB indicated 14 residues in contact with the substrates 1,6-DHN, NAR and OL. Based on the initial experiments, it was decided to change these residues to alanine and investigate their influence on the catalytic activity of NphB using the different substrates.

Four out of 14 mutants, namely Ser64Ala, Asp110Ala, Tyr121Ala and Tyr175Ala, displayed a total lack of enzymatic activity, indicating their importance for the substrate catalysis. These mutants have been suggested to play important roles in the catalytic mechanism of NphB in molecular dynamics studies. We previously suggested that residues Tyr-121 and Asp-110 form a catalytic dyad [280]. Accordingly, when mutating these residues, the resulting enzyme was inactive indicating the importance of these amino acids in NphB catalytic activity. Moreover, a π -chamber composed of Tyr-121, Tyr-216 and 1,6-DHN was identified to be stabilizing the geranyl carbo-cation [280]. When mutating the residue Tyr-216 for alanine, the mutant still displayed enzymatic activity, however, catalysis was severely reduced.

Our preliminary analysis, based on the substrate consumption of both mutants - Tyr121Ala and Asp110Ala - indicated that the substrate was consumed but no product was released (data not shown). Following the catalytic dyad hypothesis, the Tyr121Ala should trap the product by the inability of proton transfer and Asp110Ala could trap the substrate by the inability of proton subtraction. Alternatively, the affinity of GPP might have been lowered by which the reaction would be hindered as well. However, according to the stoichiometric measurements performed by Brandt *et al.* [240] carbocation formation is essential for product localization within the active center.

The residue Ser-64 has been previously associated with magnesium binding for NphB [109]. This residue was replaced by Arg in the closely related, but magnesium independent, prenyl transferases CloQ and NovQ [251, 277, 281], where it is expected, along with other residues, to take over the function normally fulfilled by magnesium. In our mutational studies, the change of this residue to an Ala abrogated enzyme activity likely because magnesium binding is disturbed.

The residues Ser-214 and Tyr-288 have also been previously discussed to play a role in substrate binding [278]. The Ser214Ala mutant was previously analyzed by *in silico* mutagenesis [278] and suggested to be involved in 1,6-DHN stabilization, subsequently leading to the formation of 2-geranyl-1,6-DHN. Our results indicated that that Ser214Ala mutant is not essential for product formation, as it did not show any reduction in activity. The NphB mutant Tyr288Ala led to a significant reduction in product formation for all tested substrates. However, our mutational analysis indicates increased involvement for 4-geranyl-1,6-DHN product formation. Tyr-288 could be important for binding and substrate orientation within the active site of NphB. Moreover, no activity was observed in the Tyr288Ala mutant when using NAR as substrate. Regarding NAR binding, this position could be important for the stabilization of the ether oxygen, as previously suggested [280]. Exchange of the Tyr-288 to Ala could therefore allow more distance between the residue and the substrate, therefore diminishing stabilization via the ether oxygen.

The mutants Gln161Ala and Gln295Ala showed an increase in production of CBG when using olivetol as substrate. Moreover, the mutant Gln161Ala showed increased activity for all tested substrates. Previous analysis suggested that Gln-161 could steer the product away from the active center, thereby, causing its fast release [278]. We [280] proposed no specific function for this residue, but the neighboring amino acid (Met-162) was mentioned to be involved in stabilization of the geranyl carbocation. Based on the observation of Yang *et al*

[278], the change of Gln-161 to Ala, thus from polar to non-polar residue, should result in the attraction of the product causing slower product release.

In summary, our mutagenesis approach provides additional information on the catalytic mechanism of NphB, highlighting the importance of several residues on substrate binding and product specificity. By using this approach, we identified the position Gln295Ala to be important for substrate specificity, as an increase in CBG formation was observed while no activity was exhibited on NAR. The mutant Val294Ala showed increased product specificity for 6-geranyl-NAR, while *O*-prenylation was completely lost.

This report provides a foundation for NphB based enzyme improvement towards various substrates. More information along with additional *in silico* and *in vitro* experiments are needed in the future to confirm the catalytic mechanism and explain in detail the influence of the mutations on the effects observed.

Materials and methods

Molecular docking of 1,6-DHN, naringenin and olivetol into NphB:

Substrates 1,6-DHN, naringenin and olivetol were constructed and molecular docking simulations were performed on wild-type NphB (Protein Data Bank accession code: 1ZB6) containing GPP in its active site, using the coordinates given by 1,6-DHN and the grid based approach CDOCKER [282, 283]. The structures were further minimized using CHARMM, consisting of 5000 steps steepest descent followed by 1000 iterations of the adopted basis-set Newton-Raphson algorithm using an energy tolerance of $0.01 \text{ Kcal.mol}^{-1}\text{\AA}^{-1}$.

NphB mutant generation:

Point mutations were generated by site directed mutagenesis using pHIS8 as template kindly obtained from S. Richards (Salk institute) encoding for NphB wild-type enzyme [284]. Primer sequences are shown in **Table 3**. PCR was conducted using equal amounts of each primer ($0.5 \text{ }\mu\text{M}$), GC buffer, a final concentration of 3 % DMSO and high fidelity phusion polymerase according to the manufacturer's protocol (Fermentas). Parental template was removed using FastDigest® DpnI (Fermentas) and subsequently transformed into *E. coli* DH5 α . Kanamycin ($30 \text{ }\mu\text{g/ml}$) was used for plasmid maintenance. Plasmids were extracted from single colonies using Qiagen plasmid purification kit (Qiagen) according to the manufacturer's instructions. Mutations were verified using DNA sequencing (Macrogen). For protein expression, correct clones were introduced into *E. coli* BL21.

NphB expression and purification:

E. coli BL21, containing pHIS8 (encoding for wild type NphB) and mutants constructed in the same plasmid, was grown in LB broth supplemented with kanamycin ($30 \text{ }\mu\text{g/ml}$) and glucose (2 %) at 37°C . Overnight cultures were used to inoculate 2XTY broth supplemented with kanamycin ($30 \text{ }\mu\text{g/ml}$) at a starting $\text{OD}_{600} = 0.1$. After incubation at 37°C , at $\text{OD}_{600} = 0.5$, protein expression was induced with a final concentration of 0.5 mM IPTG. After induction, cultures were subsequently incubated for 18 h at 25°C .

Bacterial cells were harvested using centrifugation and the pellets were resuspended in Histag binding buffer (20 mM Tris/HCl, pH 8, 20 mM imidazole, 500 mM NaCl, 0.5 % (w/v) Tween20, 10% (w/v) glycerol) (10 ml/g pellet). Cells were lysed using 3 rounds of sonication (20% intensity, 30 seconds, 1 second pulse with 1 second brake). After centrifugation to obtain cell-free extracts, the supernatants were passed through a $0.22 \text{ }\mu\text{M}$ filter.

A Biorad duo flow system was used for automated isolation of the mutants using a Ni-NTA agarose column (biorad). Protein was washed using Histag binding buffer without Tween 20. NphB and mutants were eluted with a linear gradient of imidazole ranging from 20 mM to 500 mM. Eluted proteins were mixed with thrombin (1 U/mg) to remove the HisTag and applied to a dialysis tube (cut-off 10 kDa). Dialysis buffer (50 mM Tris/HCl, pH 7.4, 1 mM DTT) was refreshed every hour for three times, and two extra buffer replacements were applied after 12 hours and 24 hours, respectively. Subsequently, another round of Ni-NTA purification was used to increase the purity of thrombin-cleaved NphB. This was further purified using a benzamidine column according to the manufacturer's instructions and the flow-through concentrated (cut-off 10 kDa). SDS-PAGE and western blot (using His detectorTM Nickel-AP (KPL)) were used for quality control. Obtained proteins had a purity of $\geq 95\%$ as shown by SDS-PAGE (Invitrogen, UK) and Coomassie staining.

Table 3. Primer sequences used for mutagenesis. Altered codon is underlined and altered nucleotides indicated in bold.

| Mutant | Primer site (5'→3') |
|------------------|--|
| Val47Ala | GTC GAG GGC GGC AGC <u>GCC</u> GTC GTC TTC TCC ATG |
| Ser64Ala | C ACG GAA CTG GAC TTC <u>GCC</u> ATC TCG GTG CCG ACC |
| Asp110Ala | CC ATG TTC GCC ATC <u>GCC</u> GGC GAG GTC ACC |
| Tyr121Ala | GGC TTC AAG AAG ACG <u>GCC</u> GCC TTC TTC CCC ACC |
| Phe123Ala | AAG AAG ACG TAC GCC <u>GCC</u> TTC CCC ACC GAC AAC |
| Thr126Ala | TAC GCC TTC TTC CCC <u>GCC</u> GAC AAC ATG CCC GGC |
| Gln161Ala | GGT CTG GAC AAG GTC <u>GCG</u> ATG ACG TCG ATG GAC |
| Tyr175Ala | CGG CAG GTC AAC CTC <u>GCC</u> TTC AGC GAG CTG AGC |
| Ser177Ala | GTC AAC CTC TAC TTC <u>GCC</u> GAG CTG AGC GCG CAG |
| Ser214Ala | TGC AAG CGC TCC TTC <u>GCG</u> GTC TAC CCC ACC CTC |
| Tyr216Ala | CGC TCC TTC TCG GTC <u>GCC</u> CCC ACC CTC AAC TGG |
| Tyr288Ala | TAC AAG CTG GGC GCG <u>GCC</u> TAC CAC ATC ACC GAT |
| Val294Ala | TAC CAC ATC ACC GAT <u>GCC</u> CAG CGC GGA CTG CTG |
| Gln295Ala | CAC ATC ACC GAT GTC <u>GCG</u> CGC GGA CTG CTG AAG |

Analysis of products for specific activity and substrate dependency:

The specific activity assay was performed 3 times in a 20 μ l reaction volume (50 mM Tris/HCl, 5 mM MgCl₂, 0.5 mM aromatic substrate (1,6-DHN, NAR and OL), 15 μ M enzyme

and 2 mM GPP) for 1 h at 30 °C. Selected mutants (10 µmol) were tested at different aromatic substrate concentrations (0, 0.125, 0.25, 0.5 and 1 mM) and constant GPP (2 mM) concentration. Samples were incubated for 5 min (1.6-DHN) or 20 min (olivetol). The reactions were stopped by addition of an equal volume of methanol containing 4-hydroxy benzoate (Sigma-Aldrich). After 5 min incubation on ice, samples were centrifuged at full speed for 30 min. Subsequently the supernatants were collected in HPLC vials for further product analyses. All reactions were corrected for the content of 4-hydroxy benzoate. Product analysis was conducted on an agilent 1200 series UPLC combined with an agilent PDA. Phase A consisted of Millipore water containing 0.1 % TFA (spectroscopic grade, Sigma Aldrich), while Phase B consisted of MeCN containing 0.1 % TFA. The flow was kept constant at 0.9 mL/min. From 0 min till 0.4 min the gradient was kept constant at 70 % phase A. From 0.4 min till 3 min a gradient from 70 % to 15 % of phase A was used, followed by a constant phase A (15 %) for 1min. Thereafter the gradient returned to the starting condition within 0.5 min and kept constant for 1.5 min.

LC-MS analysis:

All products were confirmed using high resolution-mass spectroscopy (Institute for environmental Research (INFU)). The HPLC system from Agilent Technologies (Binary SL, Series 1200, USA) consisted of a pump, an auto sampler, a diode array detector and a temperature-controlled column oven. The products were ionized via HESI (heated ESI) system at atmospheric pressure. All the identifications were carried out in full scan mode in the range of m/z = 130 to 1000. Separation occurred using a C18 Gravity column (50 mm long x 4 mm inner diameter, particle size: 1.8 µm) obtained from Macherey-Nagel. To prevent clotting an appropriate guard column was placed in front of the separation column. The flow rate constant at 0.3 ml / min. The solvent system consisted of Milli-Q water containing 0.1 % formic acid (A) and acetonitrile containing 0.1 % formic acid (B). The following gradient was used (percentages are filled till 100 % using solvent B): From 0 to 1 minute: 70 % A , from 1 to 10 minutes: linear gradient from 70 % A to 10 % A . From 10 to 12 minutes 10 % A, after that the column was brought back to the initial conditions within 8 minutes followed by equilibration at isocratic concentration of 70 % A. Data analysis occurred using Excalibur software version 2.0.7 (Thermo Scientific, USA).

You can't just leave out one part; the bread won't rise if the yeast isn't there.

- *Holly Near*